Chemistry–A European Journal
Research Article
doi.org/10.1002/chem.202402705
Chemistry Europe
European Chemical Societies Publishing
www.chemeurj.org

Hot Paper

Decarboxylative Alkylation of Carboxylic Acids with Easily Oxidizable Functional Groups Catalyzed by an Imidazole-Coordinated Fe_3 Cluster under Visible Light Irradiation

Sota Tamaki,[a] Tetsuro Kusamoto,[a] and Hayato Tsurugi*[b]

Decarboxylative alkylation of carboxylic acids with easily oxidizable functional groups such as phenol and indole functionalities was achieved using a catalytic amount of basic iron(III) acetate, $Fe(OAc)_2(OH)$, in the presence of benzimidazole under 427 nm LED irradiation. Kinetic analyses of this catalytic reaction revealed that the reaction rate is first-order in alkenes and is linearly correlated with the light intensity; the faster reaction rate for the benzimidazole-ligated species was consistent with the increased absorbance in the visible light region. Wide functional group tolerance for the easily oxidizable groups is ascribed to the weak oxidation ability of the *in situ*-generated oxo-bridged iron clusters compared with other iron(III) species.

Decarboxylation of naturally occurring carboxylic acids provides numerous advantages in synthetic organic chemistry due to the facile generation of multi-functionalized organic radicals by removing CO_2 from the carboxyl groups for further C–C or heteroatom bond-forming reactions.[1] The utilization of multi-functionalized alkyl chains reduces subsequent reaction steps in complex molecular synthesis. Naturally occurring carboxylic acids are inexpensive, easily accessible, and environmentally friendly, as CO_2 is the main byproduct and other byproducts are minimally harmful. Thus, selective conversion of the carboxyl moiety while preserving other functional groups enhances their usefulness as key intermediates in multi-step synthesis.[2] In fact, single-electron oxidation of carboxylate anions is a waste-free approach for decarboxylation, but the overpotential required for the oxidation process can induce the degradation of easily oxidizable functional groups attached to multi-functionalized carboxylic acids.[3] In this context, derivatization of carboxylic acids to more usable species such as Barton esters, NHPI-esters, and iodobenzene dicarboxylates allows for the use of multi-functionalized carboxylic acids as sources of carboxyl radicals due to their functional group stability during the generation of carboxyl radicals.[4] A large amount of reaction waste is produced from the specific ester or iodobenzene functionalities, however, following radical formation (Figure 1a). Alternatively,

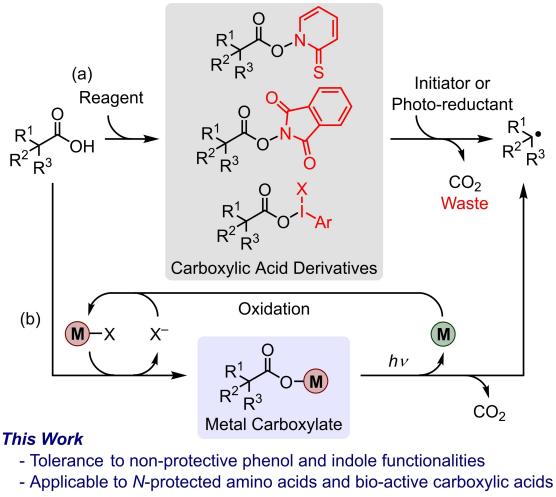

Figure 1. Decarboxylation pathways from carboxylic acids for generating organic radicals.

activation of oxime esters *via* energy transfer has recently been developed,[5] in which both of alkyl radicals and iminyl radicals are generated, leading to bifunctionalization of alkenes and (hetero)arenes with high atom economy after radical addition and radical-radical coupling sequences.[5b,c]

Photolysis of metal carboxylate complexes produces less waste and preserves functional groups because it does not require pre-treatment of carboxylic acids or external oxidants harmful to easily oxidizable groups (Figure 1b).[1a,6] In fact, photo-excitation of high-valent metal carboxylate complexes such as cerium(IV),[7] iron(III),[8] and copper(II)[9] promotes homolysis of the metal-carboxylate covalent bond to afford carboxylate radicals *via* ligand-to-metal charge transfer (LMCT). Several catalytic systems composed of iron(III) complexes, carboxylic acids, and alkenes have been reported for decarboxylative alkylation under blue LED irradiation; however, carboxylic acids with phenols, thioanisoles, alcohols, indoles, and electron-rich (hetero)aromatic rings, which are often found in naturally occurring carboxylic acids, remain problematic for

[a] S. Tamaki, T. Kusamoto
Department of Chemistry, Graduate School of Engineering Science, Osaka University, Toyonaka, Osaka, Japan
[b] H. Tsurugi
Department of Applied Chemistry, Graduate School of Engineering, Osaka University, Suita, Osaka, Japan; Innovative Catalysis Science Division, Institute for Open and Transdisciplinary Research Initiatives (ICS-OTRI), Osaka University, Suita, Osaka, Japan
E-mail: tsurugi@chem.eng.osaka-u.ac.jp

Supporting information for this article is available on the WWW under https://doi.org/10.1002/chem.202402705

decarboxylative transformation due to their low compatibility with high-valent metal complexes in the reaction mixture.[8f,p] Thus, the development of high-valent photocatalysts with weak oxidation ability and efficient photo-responsivity is highly desirable to establish decarboxylative functionalization as a major tool in organic synthesis using naturally occurring compounds. Herein, we report on decarboxylative C–C bond formation of multi-functionalized carboxylic acids catalyzed by iron salts under blue LED irradiation. A wide variety of phenol- and indole-containing carboxylic acids were applicable to form the decarboxylative alkylation products, in which benzimidazole-coordinating oxo-bridged iron clusters served as photo-responsive catalysts. This is the first example of transforming non-protected phenol- and indole-containing carboxylic acids in decarboxylative functionalization reactions.

We started by searching for an effective ligand for decarboxylative alkylation of 4-hydroxyphenylacetic acid (**1a**) as a model substrate with electron-deficient alkene **2a** under Ar with 427 nm LED irradiation at room temperature in MeCN using basic iron(III) acetate as a catalyst, and the results are summarized in Table 1. We found that benzimidazole (**L1**) was the optimal ligand for this reaction, giving the decarboxylative alkylated product **3aa** in excellent yield in 24 h (entry 1). In the absence of any ligands, **3aa** was generated in only 58% yield under the same reaction conditions (entry 2), though the final yield reached 96% after 72 h without degradation of the phenol moiety under a prolonged reaction time (entry 3). 1-Methylbenzimidazole (**L2**) and 4-phenylimidazole (**L3**) also served as good ligands, affording **3aa** in high yields (entries 4 and 5), whereas no improvement of the catalytic activity was observed for 2-phenylimidazole derivatives (**L4** and **L5**, entries 6 and 7). When *N*-heterocyclic carbene ligand **L6** was added to the reaction mixture, no positive effect was observed (entry 8); we thus ruled out the generation of carbenes from **L1**–**L3**. Although imidazole (**L7**) showed a positive effect, its chelating variant, 2,2′-biimidazole (**L8**), was ineffective under the reaction conditions (entries 9 and 10). Pyridine derivative **L9** exhibited less positive effect compared with imidazole derivatives in this catalytic reaction (entry 11). In addition, other iron sources were less active than the basic iron(III) acetate (Table S4). By changing the light source with a shorter or longer wavelength, the yield of **3aa** was low under the same reaction conditions, probably due to degradation of the phenol moiety with higher energy light (370 nm and 390 nm) and a slow reaction rate at the longer wavelength (467 nm and 525 nm) (Table S5). In this iron(III)-catalyzed decarboxylative alkylation with carboxylic acids, a simple phenol derivative was tolerant, even when added to the decarboxylative alkylation with 4-fluorophenylacetic acid (Figure S1 and Table S1); in fact, the positive effect of an imidazole derivative was found in the additive screening using a functional group evaluation kit (Figure S2 and Table S2).[10]

Table 1. Ligand screening for decarboxylative alkylation of **1a** with **2a**.[a]

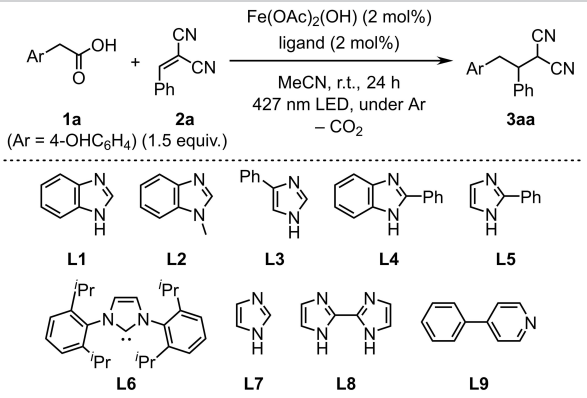

entry	ligand	yield [%][b]	entry	ligand	yield [%][b]
1	**L1**	95 (90)[c]	7	**L5**	53
2	none	58	8	**L6**	56
3[d]	none	96	9	**L7**	87
4	**L2**	94	10	**L8**	60
5	**L3**	89	11	**L9**	74
6	**L4**	61			

[a] Reaction conditions: **1a** (0.300 mmol), **2a** (0.450 mmol), $Fe(OAc)_2(OH)$ (2 mol%), ligand (2 mol%), MeCN (3.0 mL), under Ar. Irradiated with 427 nm LED (distance between the light source and the test tube, 5 cm). [b] Determined by ^1H NMR using 1,3,5-trimethoxybenzene as an internal standard. [c] Isolated yield. [d] 72 h.

With the optimal iron-photocatalyst system in hand, we screened the substrate scope with phenol and indole groups (Table 2). 3-Hydroxyphenylacetic acid (**1b**) showed high reactivity even without **L1** to give the desired product **3ba** in 95% yield, whereas the use of 2-hydroxyphenylacetic acid (**1c**) resulted in a lower yield of **3ca**. 3-Substituted-4-hydroxyphenylacetic acid **1d**–**i** were applicable to produce the corresponding alkylated products **3da**–**ia** in excellent to moderate yields for both electron-donating and -withdrawing substituents. Generally, synthesis of the corresponding NHPI-esters from carboxylic acids with a phenol group is challenging because esterification of the phenol group concomitantly proceeds under the reaction conditions; thus, this is a useful method to utilize phenol-containing carboxylic acids. Furthermore, 3-indoleacetic acid (**1j**) was suitable to give **3ja** in 96% yield. In contrast, carboxylic acids having phenol and indole groups at the β-position were less reactive, giving **3ka** and **3la** in moderate to low yields. Encouraged by the success of simple carboxylic acids with phenol and indole functionalities, we applied amino acids and bioactive molecules as multi-functionalized carboxylic acids. *N*-Boc and *N*-benzoyl-glycine (**1m** and **1n**) afforded the corresponding products **3ma** and **3na** in moderate yields. Other *N*-protected amino acids having phenol, indole, and thioether moieties were all tolerated under the reaction conditions to give **3oa**–**qa** in high to moderate yields without deprotection of the nitrogen atom, though the decarboxylative alkylation product was not observed for non-protected variants. Drug molecules with heterocyclic moieties such as bendazac (**1r**) and indomethacin (**1s**) were also applicable to produce **3ra** and **3sa** in high yields, respectively.

We further checked alkene substrates, and the results are summarized in Table 3. Methylenemalononitrile **2b** with a phenol functionality at the β-position was applicable to afford

Table 2. Substrate scope of carboxylic acids.[a]

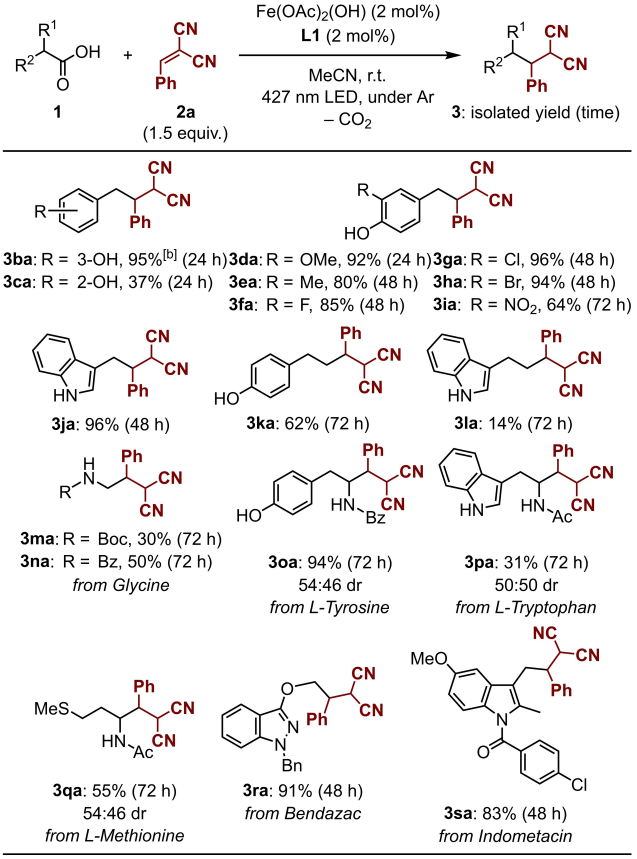

[a] Reaction conditions: **1** (0.300 mmol), **2a** (0.450 mmol), $Fe(OAc)_2(OH)$ (2 mol%), **L1** (2 mol%), MeCN (3.0 mL), under Ar. Irradiated with 427 nm LED (distance between the light source and the test tube, 5 cm). [b] Without **L1**.

Table 3. Substrate scope of alkenes.[a]

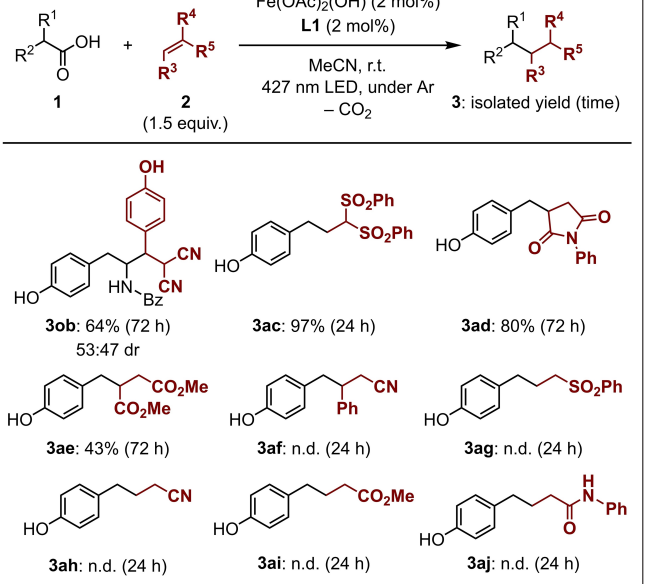

[a] Reaction conditions: **1** (0.300 mmol), **2** (0.450 mmol), $Fe(OAc)_2(OH)$ (2 mol%), **L1** (2 mol%), MeCN (3.0 mL), under Ar. Irradiated with 427 nm LED (distance between the light source and the test tube, 5 cm). n.d. = not detected.

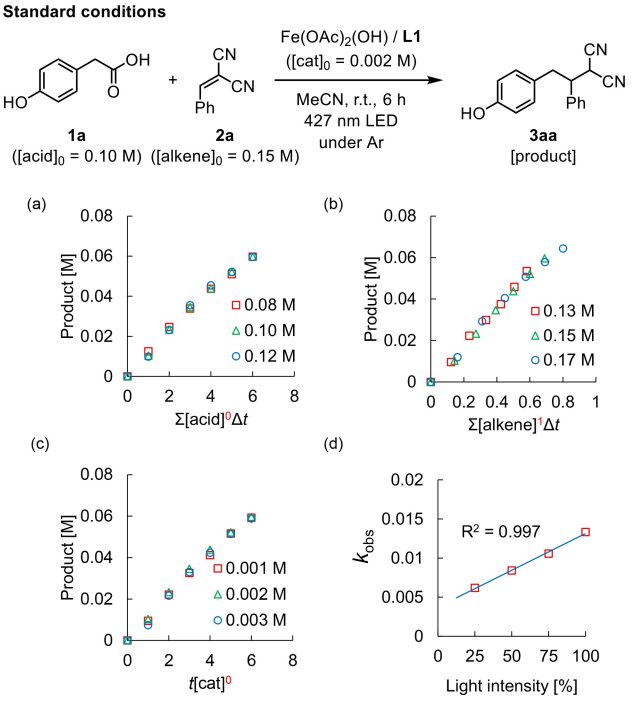

Figure 2. Variable time normalization analysis for the determination of Fe/**L1** catalytic system: (a) order on **1a** [acid]; (b) order on **2a** [alkene]; (c) order on $Fe(OAc)_2(OH)$ and **L1** [cat]; (d) order on light intensity.

3ob in moderate yield using *N*-benzoyl-protected L-tyrosine **1o**, indicating that a phenol group on the radical donors and acceptors was both tolerant in this catalytic system, though the redox potential for oxidizing substituted phenols and carboxylate anions is almost similar.[11] Decarboxylative alkylated products **3ac** and **3ad** were obtained in excellent yields, respectively, though dimethyl maleate (**2e**) was less reactive under the same reaction conditions. In contrast, alkenes **2f-j** having only one electron-withdrawing substituent on the C=C moiety were inactive under the reaction conditions. Such different reactivity is likely due to the lower reducing ability of the iron(II) center within the oxo-centered trinuclear core for carbon radicals having only one electron-withdrawing substituent (vide infra for the SET between iron(II) species and organic radicals shown in Scheme 2).

To gain insight into the reaction mechanism, we carried out a kinetic study with variable time normalization analysis, which is a graphical method for following the concentration profiles.[12] We monitored the concentration of product **3aa** under 427 nm LED irradiation with different concentrations of each reaction component, as shown in Figure 2. This catalytic system was zero-order regarding the concentrations of carboxylic acid **1a** and catalyst, while a first-order rate dependence on the concentration of alkene **2a** was observed, clearly indicating that the radical addition is the rate-determining step in the overall

catalytic cycle. Due to the lack of rate dependence on the concentration of **1a** and the iron catalyst, radical generation under the reaction conditions was reasonably rapid, but the concentration of the reactive radical in the reaction mixture depends on the light intensity: in fact, the initial reaction rate in the first half-life of **1a** and the light intensity was linearly correlated. We presumed that the lack of influence on the catalyst concentration is due to the kinetically saturated situation of the iron species under our reaction conditions, according to the dependence of the light. Our observation for this kinetic study is somewhat different from the recent report by Bunescu *et al.* on decarboxylative oxygenation with TEMPO,[8w] in which the reaction was zero-order with respect to TEMPO but first-order with respect to the carboxylic acid and iron catalyst. In contrast, our reaction involves radical addition to alkenes, and we assume that the radical coupling reaction between organic radicals and TEMPO in their system occurs so quickly that it does not affect the reaction rate, which explains the zero-order dependence on TEMPO. The reaction rate in their system, however, was limited by the availability of catalytically active iron(III) species necessary for the homolysis of the iron(III) – carboxylate bond.

We further elucidated the iron(III) complex relevant to the photo-responsive species. After mixing basic iron(III) acetate, excess amounts of **1a**, and **L1** in MeCN, we found the formation of **L1**-coordinated trinuclear iron(III) clusters, $Fe^{III}_3O(OCOR)_7(\mathbf{L1})_n$[13a] (R = $CH_2C_6H_4OH$, n = 0–3, Figure 3a), as the major species in the ESI-MS measurement, though multiple iron(III) carboxylate clusters were generated without **L1**. This trinuclear cluster formation was very rapid within a few minutes, indicating that the trinuclear cluster is the photo-responsive species in this catalytic reaction. In fact, basic iron(III) acetate contains an oxo-bridged trinuclear structure,[14] and thus, the ligand exchange reaction of the acetate to 4-hydroxyphenylacetate occurs in the presence of **L1** without decomposition of the oxo-bridged trinuclear core. After photo-irradiation for 30 minutes, iron(II)-containing clusters of $Fe^{III}_{3-n}Fe^{II}_nO(OCOR)_{7-n}$ (n = 1–3) and $Fe^{II}_2(OCOR)_4(OH_2)_3$[13b] were detected, indicating the photo-reduction of the iron(III) center along with the corresponding carboxyl radicals (Figure S10). The superiority of the **L1**-coordination on the catalytic performance is ascribed to the increased absorption coefficient in the visible light region compared to that without **L1** (Figure 3b): due to first-order dependence on light intensity for the catalytic performance, increased absorption by the **L1**-coordination improved the photo-responsivity for homolytic cleavage of the iron(III)-carboxylate bond. Lower amounts of **L1** under the optimized reaction conditions resulted in decreasing the product yields, which was also relating to the absorption coefficient of the catalytically active species (Table S7 and Figure S14). It is interesting to note that absorbance in the UV-vis absorption spectrum for the **L9**-containing mixture was in between the two spectra (Figure 3b), which is consistent with the importance of the light intensity and absorption coefficient for the homolytic cleavage process. No ligand-coordinated species for **L4** – **L6** and **L8** was detected in the ESI-MS spectra, which is also consistent with the absence of a ligand effect on the catalytic performance.

We carried out time course analyses of this decarboxylative alkylation reaction using some 4- or 3- substituted arylacetic acids, and the Hammett plot based on the competitive study for the consumption of the substrate is shown in Figure 4.[15] The reaction was faster for electron-rich arylacetic acids such as methoxy- and methyl-substituted arylacetic acids while the electron-deficient substrates were slow; electron-richness of the radical center affected the radical addition rate to electron-deficient alkene **2a**, consistent with the first-order dependence on the alkene concentration. 4-Hydroxy one **1a**, however, was the exception to the trend. In fact, monitoring the reaction

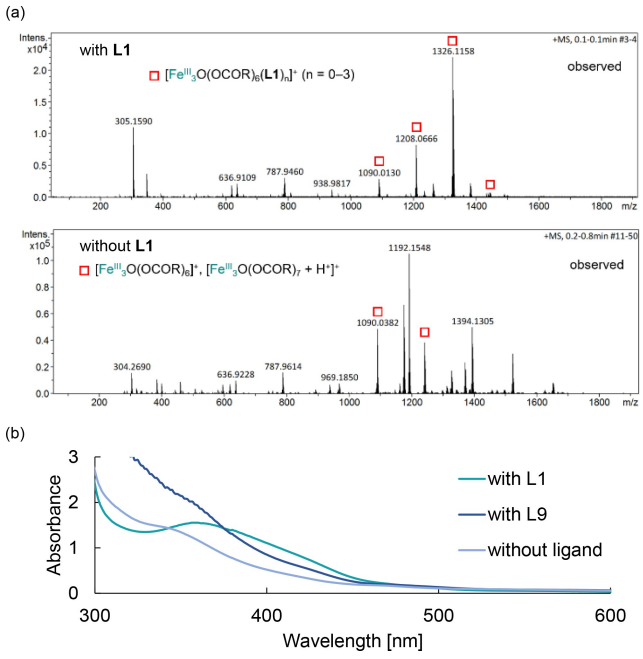

Figure 3. Spectroscopic measurement of the intermediates in the catalytic mixture: (a) ESI-MS spectra of trinuclear iron(III) cluster w/wo **L1**; (b) UV-vis absorption spectra of catalytic reaction mixtures w/wo **L1** and with **L9**.

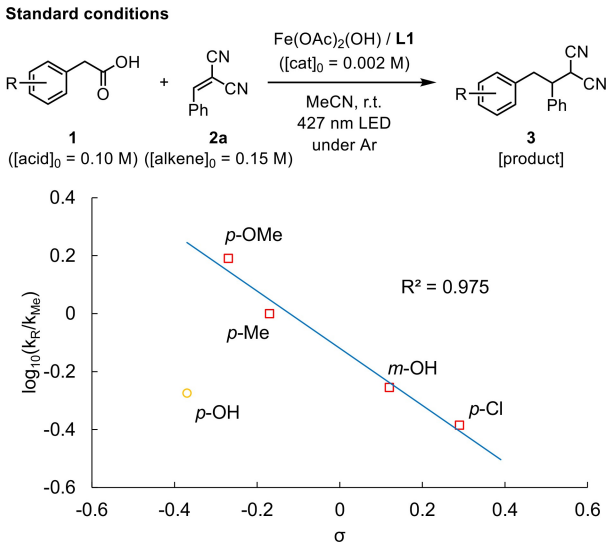

Figure 4. Hammett analysis of the decarboxylative alkylation of **1** with **2a**.

mixture using **1 a** by ESI-MS showed one characteristic signal for quinone methide (QM)-coordinating Fe_3 clusters **IV**, $[Fe_3O(OCOR)_6(\mathbf{L1})_n(QM)]^+$ (n = 1,2) (Figure S10). Reaction sequences for the formation of **IV** are explained as follows (Scheme 1); photo-irradiation of the iron(III) cluster generates carboxyl radical **I**, followed by decarboxylation, which gives 4-hydroxybenzyl radical **II**. Subsequently, hydrogen abstraction of the O–H moiety by **I** produces QM along with **1 a**, in which the low bond dissociation energy of O–H in **II** is the key factor.[16] Coordination of QM to iron(III) species produces **IV** in the reaction mixture, while coordination to iron(II) species forms **III**, followed by protonation with **1 a** to regenerate iron(III) carboxylate and **II**, which might be the reason for the slow reaction rate of **1 a** compared with other electron-rich carboxylic acids. We presumed that interconversion of **II** and QM in the presence of the iron cluster is one factor that suppresses undesired oxidative decomposition of the phenol-containing substrate. In contrast, the reactivity of *m*-OH-substituted one was fitting to the trend due to the no formation of the quinone methide-type species (Figure 4).

Based on the kinetic study and some control experiments, we propose the mechanism outlined in Scheme 2. The reaction of $Fe(OAc)_2(OH)$ with carboxylic acid **1** and benzimidazole (**L1**) affords a trinuclear iron(III) carboxylate cluster **A** with an η^1-carboxylate ligand.[13a] Then, photo-induced homolysis of the iron – (η^1-carboxylate) bond preferentially leads to the formation of iron(II)-containing cluster **B** and the corresponding carboxyl radical **C**.[9d] Subsequently, **C** undergoes decarboxylation to give the corresponding alkyl radical **D**, followed by radical addition to alkene **2 a**, forming electron-deficient organic radical **E** as the rate-determining step. In this step, QM is involved when **1 a** is used as the substrate. Then, **E** oxidizes the iron(II) center of **B** to regenerate iron(III) species **A**, during which one-electron reduction of **E** followed by protonation by the carboxylic acid affords the product **3**.[8f] Key to the tolerance of easily oxidizable functional groups is the weak oxidation ability of the **L1**-coordinated oxo-bridged iron(III) clusters formed in the reaction mixture[17]; otherwise, oxidative decomposition of the functional group is inevitable. In fact, treatment of $[Fe(O^tBu)_3]_2$ with excess amount of **1 a** in MeCN under strictly anhydrous conditions, generating $Fe(OCOR)_3$, produced a black precipitate, which suggests that the phenol group is oxidized by an *in situ*-generated mononuclear iron(III) carboxylate complex having the high oxidation ability.

In summary, we successfully achieved decarboxylative alkylation of multi-functionalized carboxylic acids without the degradation of easily oxidizable functional groups such as phenol and indole groups. Key to the success is the involvement of a strongly electron-donating oxo ligand to shift the redox potential of the photo-active trinuclear iron(III) carboxylate clusters to negative compared with the oxo-free high-oxidation state iron(III) carboxylates to weaken the oxidation ability. High-valent metal species with a weak oxidant character are obtainable by constructing the oxo-bridged multi-metallic scaffold, which is an important finding for expanding the substrate applicability to various naturally occurring carboxylic acids. Further catalyst development on this decarboxylative transformation under photo-irradiation is ongoing in our laboratory.

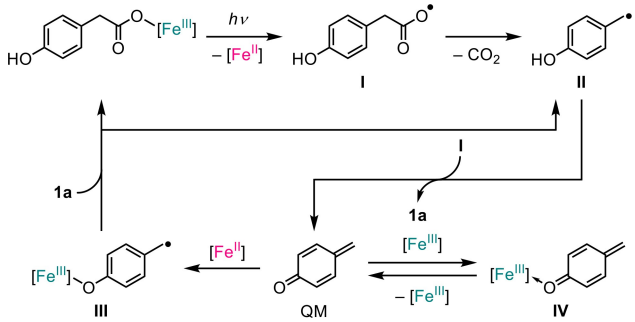

Scheme 1. Reaction sequence for the formation of quinone methide (QM).

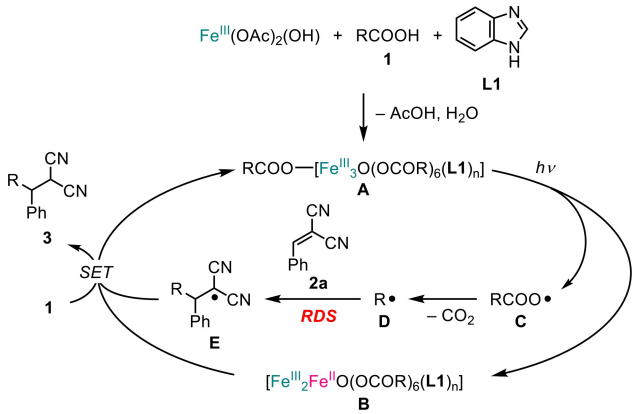

Scheme 2. Plausible mechanism of decarboxylative alkylation of carboxylic acids catalyzed by trinuclear iron clusters.

Supporting Information Summary

Additional supporting information can be found online in the Supporting Information section at the end of this article.

Acknowledgements

H.T. acknowledges the financial support by JSPS KAKENHI grant Nos. JP24H01853 (Green Catalysis Science for Renovating Transformation of Carbon-Based Resources), JP22H05365 (Digitalization-driven Transformative Organic Synthesis), and JP24 K01486 (Grant-in-Aid for Scientific Research on Innovative Areas (B)). H.T. also thanks to the financial support by Hosokawa Powder Technology Foundation (Grant Number HPTF21114). S.T. thanks the financial support by the JSPS Research Fellowships for Young Scientists.

Conflict of Interests

The authors declare no conflict of interest.

Data Availability Statement

The data that support the findings of this study are available in the supplementary material of this article.

Keywords: Decarboxylation · Iron · Homolysis · Photo-catalyst

[1] a) S. Gavelle, M. Innocent, T. Aubineau, A. Guérinot, *Adv. Synth. Catal.* **2022**, *364*, 4189–4230; b) L. Li, Y. Yao, N. Fu, *Eur. J. Org. Chem.* **2023**, *26*, e202300166.
[2] a) S. Mondal, S. Chowdhury, *Adv. Synth. Catal.* **2018**, *360*, 1884–1912; b) L. R. Malins, *Peptide Science* **2018**, *110*, e24049.
[3] a) L. Chu, C. Ohta, Z. Zuo, D. W. C. MacMillan, *J. Am. Chem. Soc.* **2014**, *136*, 10886–10889; b) K. Maeda, H. Saito, K. Osaka, K. Nishikawa, M. Sugie, T. Morita, I. Takahashi, Y. Yoshimi, *Tetrahedron* **2015**, *71*, 1117–1123; c) S. Bloom, C. Liu, D. K. Kölmel, J. X. Qiao, Y. Zhang, M. A. Poss, W. R. Ewing, D. W. C. MacMillan, *Nat. Chem.* **2018**, *10*, 205–211.
[4] a) M. F. Saraiva, M. R. C. Couri, M. L. Hyaric, M. V. de Almeida, *Tetrahedron* **2009**, *65*, 3563–3572; b) S. K. Parida, T. Mandal, S. Das, S. K. Hota, S. D. Sarkar, S. Murarka, *ACS Catal.* **2021**, *11*, 1640–1683; c) J. E. Leffler, L. J. Story, *J. Am. Chem. Soc.* **1967**, *89*, 2333–2338; d) J. I. Concepción, C. G. Fransicsco, R. Freire, R. Hernández, J. A. Salazar, E. Suárez, *J. Org. Chem.* **1986**, *51*, 402–404; e) J. Xie, P. Xu, H. Li, Q. Xue, H. Jin, Y. Cheng, C. Zhu, *Chem. Commun.* **2013**, *49*, 5672–5674; f) Y. Liang, X. Zhang, D. W. C. MacMillan, *Nature* **2018**, *559*, 83–88.
[5] a) T. Patra, S. Mukherjee, J. Ma, F. Strieth-Kalthoff, F. Glorius, *Angew. Chem. Int. Ed.* **2019**, *58*, 10514–10520; *Angew. Chem.* **2019**, *131*, 10624–10630; b) T. Patra, P. Bellotti, F. Strieth-Kalthoff, F. Glorius, *Angew. Chem. Int. Ed.* **2020**, *59*, 3172–3177; *Angew. Chem.* **2020**, *132*, 3198–3203; c) G. Tan, M. Das, H. Keum, P. Bellotti, C. Daniliuc, F. Glorius, *Nat. Chem.* **2022**, *14*, 1174–1184.
[6] a) H. Tsurugi, K. Mashima, *J. Am. Chem. Soc.* **2021**, *143*, 7879–7890; b) Y. Abderrazak, A. Bhattacharyya, O. Reiser, *Angew. Chem. Int. Ed.* **2021**, *60*, 21100–21115; *Angew. Chem.* **2021**, *133*, 21268–21284; c) F. Juliá, *ChemCatChem* **2022**, *14*, e202200916; d) L. H. M. de Groot, A. Ilic, J. Schwarz, K. Wärnmark, *J. Am. Chem. Soc.* **2023**, *145*, 9369–9388; e) A. Reichle, O. Reiser, *Chem. Sci.* **2023**, *14*, 4449–4462.
[7] a) R. A. Sheldon, J. K. Kochi, *J. Am. Chem. Soc.* **1968**, *90*, 6688–6698; b) V. R. Yatham, P. Bellotti, B. König, *Chem. Commun.* **2019**, *55*, 3489–3492; c) K. Wadekar, S. Aswale, V. R. Yatham, *Org. Biomol. Chem.* **2020**, *18*, 983–987; d) S. Shirase, S. Tamaki, K. Shinohara, K. Hirosawa, H. Tsurugi, T. Satoh, K. Mashima, *J. Am. Chem. Soc.* **2020**, *142*, 5668–5675; e) X.-L. Lai, X.-M. Shu, J. Song, H.-C. Xu, *Angew. Chem. Int. Ed.* **2020**, *59*, 10626–10632; *Angew. Chem.* **2020**, *132*, 10713–10719; f) A. R. Tripathy, G. S. Yedase, V. R. Yatham, *RSC Adv.* **2021**, *11*, 25207–25210; g) S. Singh, N. Dagar, S. R. Roy, *Chem. Commun.* **2022**, *58*, 3831–3834; h) H.-C. Li, G.-N. Li, K. Sun, X.-L. Chen, M.-X. Jiang, L.-B. Qu, B. Yu, *Org. Lett.* **2022**, *24*, 2431–2435; i) N. Dagar, S. Singh, S. R. Roy, *J. Org. Chem.* **2022**, *87*, 8970–8982; j) Y. Wang, L. Li, N. Fu, *ACS Catal.* **2022**, *12*, 10661–10667; k) X.-L. Lai, M. Chen, Y. Wang, J. Song, H.-C. Xu, *J. Am. Chem. Soc.* **2022**, *144*, 20201–20206; l) T. Kawakami, S. Tamaki, S. Shirase, H. Tsurugi, K. Mashima, *Inorg. Chem.* **2022**, *61*, 20461–20471; m) Y. Xu, P. Huang, Y. Jiang, C. Lv, P. Li, J. Wang, B. Sun, C. Jin, *Green Chem.* **2023**, *25*, 8741–8747; n) J. Lu, Y. Yao, L. Li, N. Fu, *J. Am. Chem. Soc.* **2023**, *145*, 26774–26782; o) R. Guan, G. Chen, E. L. Bennett, Z. Huang, J. Xiao, *Org. Lett.* **2023**, *25*, 2482–2486; p) M. Wang, D. Wang, K. Xu, C. Zeng, *Catal. Sci. Technol.* **2024**, *14*, 1037–1042.
[8] a) C. A. Parker, *Proc. R. Soc. Lond. A* **1953**, *220*, 104–116; b) C. G. Hatchard, C. A. Parker, *Proc. R. Soc. Lond. A* **1956**, *235*, 518–536; c) A. Sugimori, T. Yamada, *Chem. Lett.* **1986**, *15*, 409–412; d) A. Sugimori, T. Yamada, *Bull. Chem. Soc. Jpn.* **1986**, *59*, 3911–3915; e) Z. Li, X. Wang, S. Xia, J. Jin, *Org. Lett.* **2019**, *21*, 4259–4265; f) G. Feng, X. Wang, J. Jin, *Eur. J. Org. Chem.* **2019**, *2019*, 6728–6732; g) S. Xia, K. Hu, C. Lei, J. Jin, *Org. Lett.* **2020**, *22*, 1385–1389; h) K. Niu, P. Zhou, L. Ding, Y. Hao, Y. Liu, H. Song, Q. Wang, *ACS Sustainable Chem. Eng.* **2021**, *9*, 16820–16828; i) Y. Zhang, J. Qian, M. Wang, Y. Huang, P. Hu, *Org. Lett.* **2022**, *24*, 5972–5976; j) J.-L. Tu, H. Gao, M. Luo, L. Zhao, C. Yang, L. Guo, W. Xia, *Green Chem.* **2022**, *24*, 5553–5558; k) H. Kang, S. An, S. Lee, *Org. Chem. Front.* **2023**, *10*, 5151–5757; l) M. Innocent, G. Lalande, F. Cam, T. Aubineau, A. Guérinot, *Eur. J. Org. Chem.* **2023**, *26*, e202300892; m) Y.-C. Lu, J. G. West, *Angew. Chem. Int. Ed.* **2023**, *62*, e202213055; *Angew. Chem.* **2023**, *135*, e202213055; n) K.-J. Bian, Y.-C. Lu, D. Nemoto, S.-C. Kao, X. Chen, J. G. West, *Nat. Chem.* **2023**, *15*, 1683–1692; o) A.-M. Hu, J.-L. Tu, M. Luo, C. Yang, L. Guo, W. Xia, *Org. Chem. Front.* **2023**, *10*, 4764–4773; p) N. Xiong, Y. Li, R. Zeng, *ACS Catal.* **2023**, *13*, 1678–1685; q) S. Fernández-García, V. O. Chantzakou, F. Juliá-Hernández, *Angew. Chem. Int. Ed.* **2024**, *63*, e202311984; *Angew. Chem.* **2024**, *136*, e202311984; r) M. Ding, S. Zhou, S. Yao, C. Zhu, W. Li, J. Xie, *Chin. J. Chem.* **2024**, *42*, 351–355; s) Y. Zhu, H. Gao, J.-L. Tu, C. Yang, L. Guo, Y. Zhao, W. Xia, *Org. Chem. Front.* **2024**, *11*, 1729–1735; t) X.-K. Qi, L.-J. Yao, M.-J. Zheng, L. Zhao, C. Yang, L. Guo, W. Xia, *ACS Catal.* **2024**, *14*, 1300–1310; u) J. Qian, Y. Zhang, W. Zhao, P. Hu, *Chem. Commun.* **2024**, *60*, 2764–2767; v) A. Fall, M. Magdei, M. Savchuk, S. Oudeyer, H. Beucher, J.-F. Brière, *Chem. Commun.* **2024**, *60*, 6316–6319; w) L. M. Denkler, M. A. Shekar, T. S. J. Ngan, L. Wylie, D. Abdullin, M. Engeser, G. Schnakenburg, T. Hett, F. H. Pilz, B. Kirchner, O. Schiemann, P. Kielb, A. Bunescu, *Angew. Chem. Int. Ed.* **2024**, *63*, e202403292; *Angew. Chem.* **2024**, *136*, e202403292; x) M. Innocent, C. Tanguy, S. Gavelle, T. Aubineau, A. Guérinot, *Chem. Eur. J.* **2024**, *30*, e202401252; y) Z. Song, L. Guo, C. Yang, W. Xia, *Org. Chem. Front.* **2024**, *11*, 4436–4441.
[9] a) W. Su, P. Xu, T. Ritter, *Angew. Chem. Int. Ed.* **2021**, *60*, 24012–24017; *Angew. Chem.* **2021**, *133*, 24214–24219; b) P. Xu, P. López-Rojas, T. Ritter, *J. Am. Chem. Soc.* **2021**, *143*, 5349–5354; c) P. Xu, W. Su, T. Ritter, *Chem. Sci.* **2022**, *13*, 13611–13616; d) A. Reichle, H. Sterzel, P. Kreitmeier, R. Fayad, F. N. Castellano, J. Rehbein, O. Reiser, *Chem. Commun.* **2022**, *58*, 4456–4459; e) Q. Y. Li, S. N. Gockel, G. A. Lutovsky, K. S. DeGlopper, N. J. Baldwin, M. W. Bundesmann, J. W. Tucker, S. W. Bagley, T. P. Yoon, *Nat. Chem.* **2022**, *14*, 94–99; f) N. W. Dow, P. S. Pedersen, T. Q. Chen, D. C. Blakemore, A.-M. Dechert-Schmitt, T. Knauber, D. W. C. MacMillan, *J. Am. Chem. Soc.* **2022**, *144*, 6163–6172; g) T. Q. Chen, P. S. Pedersen, N. W. Dow, R. Fayad, C. E. Hauke, M. C. Rosko, E. O. Danilov, D. C. Blakemore, A.-M. Dechert-Schmitt, T. Knauber, F. N. Castellano, D. W. C. MacMillan, *J. Am. Chem. Soc.* **2022**, *144*, 8296–8305; h) P. P. Sen, S. R. Roy, *Organometallics* **2023**, *42*, 1658–1666; i) Y. Yuan, J. Yang, J. Zhang, *Chem. Sci.* **2023**, *14*, 705–710; j) P. S. Pedersen, D. C. Blakemore, G. M. Chinigo, T. Knauber, D. W. C. MacMillan, *J. Am. Chem. Soc.* **2023**, *145*, 21189–21196.
[10] N. Saito, A. Nawachi, Y. Kondo, J. Choi, H. Morimoto, T. Ohshima, *Bull. Chem. Soc. Jpn.* **2023**, *96*, 465–474.
[11] H. G. Roth, N. A. Romero, D. A. Nicewicz, *Synlett* **2016**, *27*, 714–723.
[12] a) J. Burés, *Angew. Chem. Int. Ed.* **2016**, *55*, 2028–2031; *Angew. Chem.* **2016**, *128*, 2068–2071; b) J. Burés, *Angew. Chem. Int. Ed.* **2016**, *55*, 16084–16087; *Angew. Chem.* **2016**, *128*, 16318–16321.
[13] a) S. Supriya, K. S. Latha, S. K. Das, *Eur. J. Inorg. Chem.* **2005**, *2005*, 357–363; b) W. B. Tolman, A. Bino, S. J. Lippard, *J. Am. Chem. Soc.* **1989**, *111*, 8523–8524.
[14] L. E. Orgel, *Nature* **1960**, *187*, 504–505.
[15] C. Hansch, A. Leo, R. W. Taft, *Chem. Rev.* **1991**, *91*, 165–195.
[16] a) BDFE of OH for 4-hydroxybenzyl radical was calculated to be 47.3 kcal mol^{-1}, see Supporting Information; b) M. Lucarini, P. Pedrielli, G. F. Pedulli, S. Cabiddu, C. Fattuoni, *J. Org. Chem.* **1996**, *61*, 9259–9263.
[17] K. Nakata, A. Nagasawa, Y. Sakaki, T. Ito, *Chem. Lett.* **1989**, *18*, 753–756.

Manuscript received: July 16, 2024
Accepted manuscript online: September 3, 2024
Version of record online: October 30, 2024